Title
Estimation of Worker Fruit-Picking Rates with an Instrumented Picking Bag

Permalink
https://escholarship.org/uc/item/2gr9f0ph

Journal
Journal of the ASABE, 63(6)

ISSN
2769-3295

Authors
Fei, Zhenghao
Shepard, John
Vougioukas, Stavros G

Publication Date
2020-11-20

DOI
10.13031/trans.13981

Peer reviewed

ESTIMATION OF WORKER FRUIT-PICKING RATES WITH AN INSTRUMENTED PICKING BAG

Z. Fei, J. Shepard, S. G. Vougioukas

HIGHLIGHTS

- We designed a low-cost instrumented picking bag that can monitor the worker's fruit picking process.
- The bag can be used to estimate the worker's picking rate for better workforce management.
- The bag can also be used to estimate the accumulated fruit weight and generate a yield map for orchard management.
- The best root mean squared error over the entire measurement range was 0.36 kg (1.8% of bag capacity).

ABSTRACT.

Estimating and recording a worker's picking rate during tree fruit harvesting can provide useful information for better workforce management, orchard platform crew management, and generation of yield maps (in combination with position). A commercial picking bag was instrumented to estimate harvested fruit weight, in real-time. All electronics were placed inside an enclosure that was placed between the bag and its shoulder straps, without hindering picking motions. Electronics included: two load cells to measure the forces exerted on the straps by the bag and fruits; an Arduino microcontroller; signal conditioning circuits; data storage; wireless communication components, and inertial sensors. Software was developed for data acquisition, filtering, transmission, and storage. Two calibration models were developed to estimate fruit weight. One model (#2) utilized inertial sensor data to compensate for the picking bag's angle with respect to gravity direction, whereas the other model (#1) did not. Dynamic calibration experiments were performed over the entire weight range of the bag (0 to 20 kg), with reference objects of known weight (baseballs and fresh apples). The weight range was divided into three operating regions: light load (< 8kg), medium load (8-13kg), and heavy load (>13 kg). Results showed that model #1 performed slightly better in the light-load region, but model #2 was superior in the medium and heavy load regions, presumably due to bag angle compensation. The best root mean squared error over the entire range was achieved by model #2 and was 0.36 kg (1.8% of bag capacity). As an application case study, two bags were used by workers harvesting from a platform in a commercial apple orchard; from the data, pickers' harvesting speeds were estimated, and fruit yield distribution was calculated for one side of a tree row.

Keywords.

Fruit harvesting, Yield monitor, Electronics, Calibration, Labor.

INTRODUCTION

Practically all fresh-market fruits are harvested manually (Zhang, 2017); human pickers use tall ladders to reach fruit located at higher parts of the canopies and carry picking bags to store the harvested fruits (Figure 1a). Once their bag is full, a picker will walk to the closest bin (Figure 1b), empty the bag into the bin, and resume picking. In orchards where tree canopies are narrow and form a "fruit-wall," machine-aided or mechanized harvesting can be done; pickers harvest while standing on a mobile orchard platform, at different levels, and ladders are not needed (Figure 1c). On many platforms, pickers still use picking bags to store the harvested fruit temporarily, and unload their bag in the bin that is carried by the platform; hence, walking to a bin is also eliminated. Picking platforms with fruit conveyance mechanisms exist (eliminating the need for picking bags), such as the vacuum apple harvester from Phil Brown, Welding, Conklin, MI. However, the cost of such platforms is higher than the cost of platforms that don't have a fruit conveyance system, and their adoption has been limited.

a) **b)** **c)**

Figure 1 a) A picker on a ladder picks pears and uses a picking bag to store them; b) Pickers unload their picking bags into bins that are pre-positioned in the orchard rows; c) Pickers harvest apples from a mobile orchard platform; picking bags are used to store fruit during picking.

In both manual and machine-aided commercial harvesting, picker productivity and yield are measured by the number of bins filled per acre. Typically, the weight of a bin is only known roughly (from prior experience); i.e., it is not measured. Hence, productivity and yield are tracked at a very low spatial resolution (per acre), and in terms of bins rather than weight. Also, this information is typically available only after entire orchard blocks have been harvested, i.e., data are not available in real-time, while workers are filling their bags. Getting such information at higher spatial resolution and temporal resolutions during manual picking could drive more informed orchard and workforce management.

A relatively small number of prototype systems have been developed to better track the harvested yield of horticultural crops (Zude-Sasse et al. (2016)). Schueller et al. (1999) developed a coarse-resolution yield mapping system for hand-harvested citrus by georeferencing all filled containers/bins; each container carried approximately 400 kg of citrus (containers were not weighed). Ampatzidis et al. (2009a; 2009b) developed a yield mapping system for hand-harvested fruits, which utilized a scale on a tractor. Fruit boxes were weighed manually, and the location was recorded using RFID tags on boxes and an RFID reader with a GPS. Aggelopoulou et al. (2010) measured an apple orchard's yield by asking pickers to hand-harvest apples from groups of five adjacent trees, and by recording the GPS location of the central tree. The apples were placed in plastic bins along the tree rows and weighted afterward. Ampatzidis et al. (2013) developed a portable picker efficiency monitoring system for manually-harvested sweet cherries. A digital weighing platform was built and deployed to measure the weight of a commercial fruit bin while pickers emptied their picking bags in it. Data was logged and transmitted wirelessly to a host computer, and individual worker picking rates (kg/min) were estimated from the data. A variation of this system was built by Ampatzidis et al. (2016) to monitor picker productivity in real-time. Pickers had to manually weigh their buckets before unloading them in a bin. Colaço et al. (2015) described a yield mapping method for manually harvested crops and relied on weighing each georeferenced bin (bag) manually by the harvest team leader. Vatsanidou et al. (2014) mapped the yield of a pear orchard by having workers hand-pick pears and place them in plastic bins (one bin per five trees in a row). The bins were weighted and georeferenced using GPS.

All the above systems require that pickers perform extra operations, such as weighing their bags, which interfere with - and are expected to delay - the picking process. Also, the above systems are not applicable to machine-aided harvesting using platforms, an operation that is becoming increasingly important as labor shortages increase. Finally, the spatial and time resolutions of these systems are limited, and data are available only after entire bags or bins have been filled, but not while workers are picking fruit and placing them in their bags. The importance of real-time data streams with workers' picking rates is expected to become increasingly important, as automated - and even robotic - harvest-aid machines are developed for specialty crop production (e.g., Khosro Anjom, Vougioukas, 2019).

The objective of this study was to develop a low-cost, easy-to-use system that can measure in real-time the amount of fruit a worker has picked, without intervening with the picking process or requiring any involvement of the picker. The envisioned application scenario is pickers harvesting from a mobile platform. Since the picking bag – or picking bucket - is the standard tool used to harvest fruits in commercial harvesting operations, a commercially available picking bag was instrumented with sensors, electronics, a microcontroller, and software to provide real-time measurement of harvested fruit weight during fruit picking. This approach – of instrumenting an existing industry tool – has been used successfully in strawberry harvesting (Khosro Anjom, Vougioukas, & Slaughter, 2018), albeit that tool was not a wearable subject to contact forces – it was a wheelbarrow cart - and hence, estimating harvested yield from load cells was simpler. The main contributions of this paper are the development of a force-balance model for the picking bag, the formulation of two calibration models to estimate fruit weight from sensor data, and the performance of experiments that resulted in very small calibration errors. The rest of the paper is structured as follows. Section 2 provides a detailed description of the developed system. Section 3 presents a detailed analysis of forces acting on the picking bag during harvesting, and Section 4 presents two calibration models to estimate fruit load from sensor measurements. Section 5 presents calibration and validation procedures for the models, and Section 6 presents experimental results. Finally, Section 7 presents an application case-study, where the bags were used by pickers in a commercial apple orchard in Lodi, CA, and the data were used to monitor picking speeds and estimate fruit distribution along a side of an orchard row. Finally, Section 8 summarizes our work and discusses the main conclusions and future work.

MATERIALS AND METHODS

SYSTEM OVERVIEW

The system was developed based on a commercially available fruit picking bag (Figure 2a) (Wells & Wade Harvest Bucket Deluxe, Wenatchee, WA, USA) that is representative of picking bags used in commercial harvesting operations. During harvest, each picker carries a bag and places the picked fruit in it. When the bag is full, the picker opens up the bottom of the bag by lifting the side ropes, so that the knots that hold them in place are lifted from the side-hooks that keep them in place (Figure 2b), and lets the fruits roll gently into a bin. Then, the picker secures the side ropes to close the bottom of the bag and resumes picking. Our goal was to add load cells and instrumentation without making any changes to the bag. An aluminum enclosure/box was built with two fixed metal snaps at the top (Figure 2d) and two metal bars with holes at the bottom. The metal bars were connected to the load cells inside the box. The top of the metal box was connected to the shoulder straps, and the bottom was connected to the metal snaps of the bag (Figure 2c); no changes were made to the bag. All the add-on electronics were placed inside the metal box (Figure 2d). Electronics included an Arduino microcontroller (Arduino Pro Mini 328 - 5V/16MHz, SparkFun Electronics, Niwot, Colorado), two load cells (TAL220 10kg Straight Bar, HT Sensor Technology CO., LTD, XI'AN, China), two HX711 load cell signal conditioning amplifiers and 24-bit analog-to-digital converters (SparkFun Electronics, Niwot, Colorado), an Inertial Measurement Unit (IMU) (SparkFun 9DoF Sensor Stick LSM9DS1, SparkFun Electronics, Niwot, Colorado) for measuring rotation angles, velocities and linear acceleration, an Xbee module (XBee 1mW Trace Antenna - Series 1 (802.15.4), Digi International, Hopkins, MN) for wireless data transmission, and a data logging module (OpenLog, SparkFun Electronics, Niwot, Colorado) for logging data. Two lithium-ion batteries (18650 Cell, 2600mAh, 3.7V) were used for powering the entire system. Lab tests with the system in full operation (measuring, storing and transmitting data) showed that the system can operate continuously for 26.5 hours, which is enough for three 8-hour work shifts. If longer battery life is needed, one could replace the 5V/16MHz Arduino Pro Mini with the 3.3V/8MHz version and set the proper power-saving modes for the microcontroller and Xbee module to save energy.

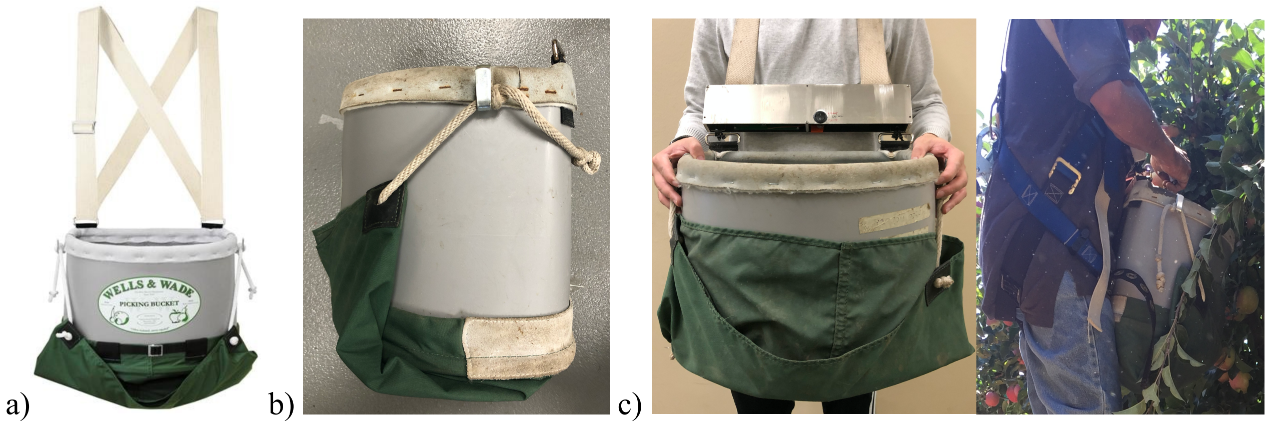

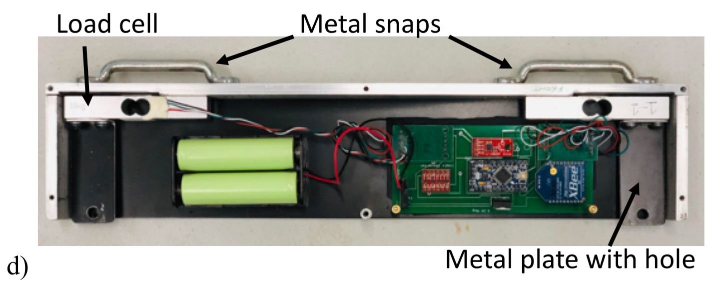

Figure 2 a) The original fruit picking bag; b) Side-view of the picking bag showing the knot holding the side rope in place; c) Instrumented picking bag with aluminum enclosure/box that contains all electronics; d) Add-on electronics inside aluminum box.

The microcontroller polls all the sensors, reads their outputs, and transmits them wirelessly in real-time – with corresponding timestamps - to a host computer, at a frequency of 10 Hz. It also logs all sensor data on the SD memory card, for off-line processing, at the same frequency. Software running on the host computer decodes the serial data received wirelessly, filters the data, first with a median filter and then with a low-pass filter, to remove outliers from impulsive noise and high-frequency noise respectively, and predicts fruit weight inside the bag based on the filtered sensor data and a prediction model. The overall hardware system diagram is shown in Figure 3 below.

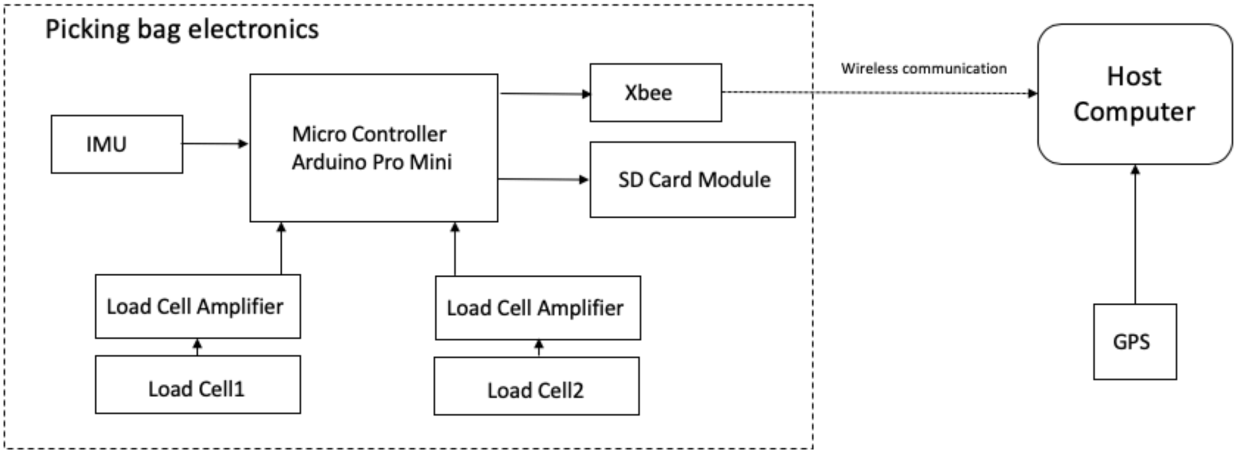

Figure 3 Hardware system diagram of the instrumented picking bag. If the bag is used by pickers on a platform, a host computer with a GPS receiver collects bag data and position data.

MICROCONTROLLER

The microcontroller in the system is an Arduino Pro Mini, which is a coin size microcontroller board with an ATmega328 processor. The advantages of this microcontroller include its tiny size, light-weight, and low power consumption, which fit for a wearable device as this picking bag; also, its processing power and I/O port are enough to support our system. The Arduino Pro Mini was programmed using the C++ language.

LOAD CELLS AND AMPLIFIER

Two straight bar load cells (TAL220) are placed between the bag and its shoulder straps. The load cells measure the forces exerted on the straps by the bag and fruits, as shown in Figure 2. The bag has a capacity of 20 kg, and typically, pickers do not exceed it (otherwise, fruits above the fill-level start falling off the bag). By construction (Figure 2), the weight of the bag is split relatively equally between the load cells. When the bag is heavy, the accelerations caused by the pickers' activities – and resulting forces on the load cells - are expected to be small. Therefore, the full measurement scale (FS) of each load cell was selected to be 10 kg (with 120% FS safe overload, and 150% FS ultimate overload); the rated error is ± 0.05% FS. The selected range was deemed adequate for the specific bag. If higher loads are expected or measured (not the case in our experiments), one can increase the safety margin by using load cells with larger FS.

An HX711 amplifier and analog-to-digital converter reads the output of each load cell, amplifies it (gains is 64, corresponding to a full-scale differential voltage of ±40 mV), and communicates with the microcontroller through the I2C protocol.

Inertial measurement unit

The LSM9DS1 IMU is placed on the back of the aluminum enclosure, as showed in Figure 4. The LSM9DS1 is a small integrated circuit chip that contains a 3-axis accelerometer, a 3-axis gyroscope, and a 3-axis magnetometer. The zero-g level offset of this chip is ±90 mg. Its programmable acceleration measurement range was set at ±4g, with acceleration sensitivity equal to 0.122 mg/LSB. When attached to a rigid body, the IMU provides the body's three acceleration components, rotational velocities, and components of the local magnetic field vector (total of nine measurements). Under static conditions, the accelerometer provides the three Euler angles of the body's weight vector with respect to an internal reference frame, i.e., body 3D pose. The IMU communicates with the microcontroller through the I2C protocol.

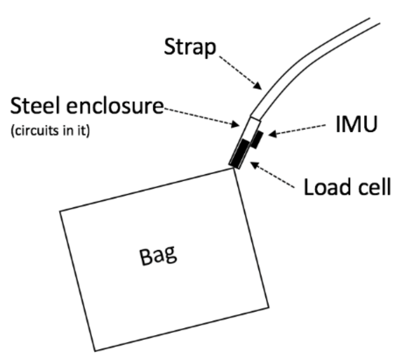

Figure 4 A sketch of the picking bag and the locations of the sensors.

Data storage and wireless transmission module

The data is transmitted wirelessly through an Xbee module to a host computer. The module is the XBee 1mW Trace Antenna - Series 1, which is low energy-consuming. It can publish serial communication to a maximum range of 100 meters. An SD card module is used to backup data and store it off-line.

Modeling the Picking Bag

Force Analysis

The force balance on the picking bag was modeled, as shown in Figure 5, to establish the relationship between the sensors' measurements and the load weight in the bag.

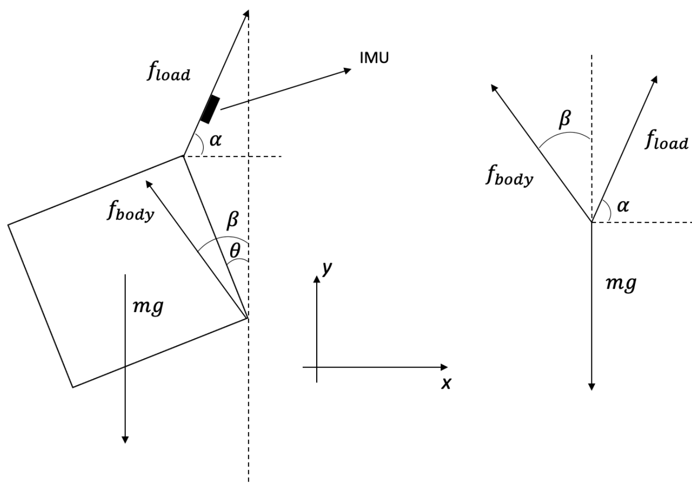

Figure 5 Force analysis of the picking bag.

Where f_{load} is the force measured by the load cells in the direction of the straps and is equal to the sum of the individual load cell forces, f_{load1}, f_{load2}, respectively. f_{body} is the total reaction force due to bag-picker contact. m is the mass of the bag and load. α is the angle of f_{load} with *x-axis* as shown above. β is the angle of f_{body} with the *y*-axis as shown above, and θ is the angle of the bag with the *y*-axis, as shown above.

Let a_x, a_y be the bag's accelerations in the *x* and *y* directions, in the inertial frame. (In the following, the absence of frame superscript means the inertia frame; the absence of subscript means the object is the bag.)

Here, it is assumed that f_{load} and f_{body} are the only external forces applied to the bag. Also, by using the current suite of sensors, there is no method to measure directly the direction and magnitude of f_{body}.

System analysis

The force balance in the *x* and y directions is: given in Eq. 1 and Eq. 2, respectively:

$$f_{load}cos\alpha - f_{body}sin\beta = ma_x \tag{1}$$

$$f_{load}sin\alpha + f_{body}cos\beta = m(a_y + g) \tag{2}$$

Solving for the reaction force from Eq. 1, and assuming $\beta \neq 0$, we get:

$$f_{body} = \frac{f_{load}cos\alpha - ma_x}{sin\beta} \tag{3}$$

By combining Eqs. 2 and 3, we get:

$$m(a_y + g) = f_{load}sin\alpha + \frac{f_{load}cos\alpha - ma_x}{sin\beta}cos\beta \tag{4}$$

The mass can be expressed as:

$$m = \frac{f_{load}(sin\alpha + cos\alpha cot\beta)}{a_y + g + a_x cot\beta} \tag{5}$$

or

$$m = \frac{(f_{load1} + f_{load2})(sin\alpha + cos\alpha cot\beta)}{a_y + g + a_x cot\beta} \tag{6}$$

ANGLE ESTIMATION

The poses of the bag and the electronics box are important information to estimate total mass. However, the roll, pitch, and yaw angles of the bag and box in the inertial frame cannot be directly measured by our sensor. The accelerometer signals of the IMU can be modeled as following (Beard & McLain, 2012)

$$y_{accel,x} = \dot{u} + qw - rv + gsin\theta_{imu} + \eta_{accel,x} \tag{7}$$

$$y_{accel,y} = \dot{v} + ru - pw - gcos\theta_{imu}sin\phi_{imu} + \eta_{accel,y} \tag{8}$$

$$y_{accel,z} = \dot{w} + pv - qu - gcos\theta_{imu}cos\phi_{imu} + \eta_{accel,z} \tag{9}$$

where y_{accel} is the reading of the IMU's accelerometer; θ_{imu}, ϕ_{imu} are the pitch and roll angles of the IMU, and *u, v, w* are velocities along the *x*, *y*, *z* axes in the IMU' s body frame. $\dot{u}, \dot{v}, \dot{w}$ are accelerations along *x, y, z* axes in IMU' s body frame; *p, q, r* are roll, pitch, yaw rates measured along the x, y, z axes in the IMU's body frame, and η is Gaussian noise.

The IMU is firmly attached to the electronics box, so the states of the IMU are also the states of the object. High-frequency Gaussian noise can be reduced significantly by applying a low pass filter to the signal. Under the assumption that the object is quasi-static ($\dot{u} = \dot{v} = \dot{w} \cong 0, u = v = w \cong 0$) and Gaussian noise has been removed, one gets the following simplified equations:

$$y_{accel,x} = gsin\theta_{imu} \tag{10}$$

$$y_{accel,y} = -gcos\theta_{imu}sin\phi_{imu} \tag{11}$$

$$y_{accel,z} = -gcos\theta_{imu}cos\phi_{imu} \tag{12}$$

The quasi-static assumption corresponds to a simplified approach to calculate roll and pitch angles in the inertial frame and then calculate α.

$$\theta_{imu} = \pi - \alpha \tag{13}$$

$$y_{accel_{imu},x} = gsin(\pi - \alpha) = gsin\alpha \tag{14}$$

$$y_{accel_{imu},y} = -gcos(\pi - \alpha)sin\phi_{imu} = gcos\alpha sin\phi_{imu} \tag{15}$$

$$y_{accel_{imu},z} = -gcos(\pi - \alpha)cos\phi_{imu} = gcos\alpha cos\phi_{imu} \tag{16}$$

$$\alpha = tan^{-1}\frac{y_{accel_{imu},x}}{\sqrt{y^2_{accel_{imu},y}+y^2_{accel_{imu},z}}} \tag{17}$$

The zero acceleration assumption will not hold during real-world harvesting when the picker is moving, and the picking bag is in direct contact with her/him; this is expected to be more pronounced when the bag contains little fruit and contact forces will cause accelerations. However, the picking bag becomes heavy as more fruit is harvested, and in practice, its acceleration and speed due to picker motion are expected to be small.

Calibration Model

Static Model Without IMU (Model #1)

We have derived an equation linking states to mass (Eq. 6); however, not all states in Eq. 6 are available. We have to make some assumptions before we use Eq. 6. Starting from the easiest solution, we can use only load cells without any IMU in our system. This solution has the lowest cost and most stable since it has minimum complexity. Also, this solution limits the information we can use and make the system less observable. The performance may be reduced if we only use load cells as sensors. Nevertheless, it is still a good model to start with.

The sensors used in this model are only the load cells. Since we have no method to measure α , β angle or estimate α_x, α_y, so we assume that α and β are constant and $\alpha_x = \alpha_y \approx 0$. By applying these assumptions to Eq. 6, we get the following Eq. 18:

$$m = \frac{(f_{load1} + f_{load2}) * (sin\alpha + cos\alpha cot\beta)}{g} \tag{18}$$

The term $(sin\alpha + cos\alpha cot\beta)$ is constant, since α and β are constant.

We can see the mass is now a linear function of measured load cell forces f_{load1}, f_{load2}.

By expanding Eq. 18, we get Eq. 19:

$$m = \frac{f_{load1} * (sin\alpha + cos\alpha cot\beta)}{g} + \frac{f_{load2} * (sin\alpha + cos\alpha cot\beta)}{g} \tag{19}$$

We constructed a linear model based on Eq. 19 to fit parameters that can give the least-squares error. Considered that two load cells may have different calibration equations, we use different c_1 and c_2 as correction coefficients and added a bias compensate factor b_0. We formalized the linear regression Eq. 20, as shown below.

$$\hat{m} = b_0 + b_1 x_1 + b_2 x_2 \tag{20}$$

The dependent variable $\hat{m}$ is the predicted mass of the bag and load. Independent variables x_1, x_2 represent f_{load1}, f_{load2}.

The parameter b_0 is the bias compensation factor, b_1 is the estimation of the term $c_1 * \frac{(sin\alpha+cos\alpha cot\beta)}{g}$, and b_2 is the estimation of the term $c_2 * \frac{(sin\alpha+cos\alpha cot\beta)}{g}$.

Static model with IMU on the Electronics Box (Model #2)

In addition to the data from the two load cells, additional data are available from the IMU sensor on the electronics box. These data can be used to estimate the α angle; however, the β angle and the bag accelerations cannot be determined from the IMU data. To improve the accuracy of the model without increasing complexity, we assume that β is constant and $\alpha_x = \alpha_y \approx 0$. By applying these assumptions to Eq. 6, we get Eq. 21:

$$m = \frac{f_{load1}*(sin\alpha+cos\alpha cot\beta)}{g} + \frac{f_{load2}*(sin\alpha+cos\alpha cot\beta)}{g} \tag{21}$$

Where $cot\beta$ is a constant and α can be estimated using Eq. 17

After expanding Eq. 21, we get Eq. 22:

$$m = \frac{f_{load1}sin\alpha}{g} + \frac{f_{load1}cos\alpha cot\beta}{g} + \frac{f_{load1}sin\alpha}{g} + \frac{f_{load1}cos\alpha cot\beta}{g} \tag{22}$$

The mass is a linear function of four independent variables. A linear regression equation can be expressed as follows:

$$\widehat{m} = b_0 + b_1x_1 + b_2x_2 + b_3x_3 + b_4x_4 \tag{23}$$

The dependent variable $\widehat{m}$ is the predicted mass of the bag and fruit yield. Independent variable x_1 corresponds to the term $f_{load1}sin\alpha$, independent variable x_2 corresponds to the term $f_{load2}sin\alpha$, independent variable x_3 corresponds to the term $f_{load1}cos\alpha$, and independent variable x_4 corresponds to $f_{load2}cos\alpha$. The parameter b_0 is the bias compensation factor, b_1 is the estimation of the term $\frac{c_1}{g}$, b_2 is the estimation of the term $\frac{c_2}{g}$, b_3 is the estimation of $\frac{c_1cot\beta}{g}$, and b_4 is the estimation of $\frac{c_2cot\beta}{g}$., where c_1 and c_2 are the correction coefficients for the load cells.

EXPERIMENTAL DESIGN

DATA COLLECTION

Calibration dataset: Reference object (baseball) batch-drop dataset

Dynamic calibration was performed in the lab over the entire weight range. Baseballs were used as reference objects to perform calibration because their weight is standardized; each ball has mass equal to 0.14239 ± 0.0008 kg.

The following procedure was followed for calibration.

1. A person put on the bag and all baseballs were placed on the surface of a table, at chest height.
2. Five baseballs were placed together - as a batch – in the bag to produce a stair-case weight signal that was used as ground truth. Each weight level differed from the previous one by 0.71195 ± 0.004 kg.
3. The edge of the bag was manually pushed to generate an easily-detectable impulse signal for separating batches.
4. Picking-like movements (move upper body and arms to reach 'fruits') were performed continuously to mimic apple picking on a harvesting platform.
5. Steps 1-4 were repeated until the bag was full.

Eight bags were filled using the above procedure by eight people with different heights and body weights. Figure 6 a) and b) show the example trace of the ground truth signal and the load cell signals. Figure 6 c) Shows the mean of the estimated α angle and its standard deviation with respect to the load weight, from all experiments. The figure suggests that the α angle was slightly decreasing as the weight of the bag increased and the deviation (fluctuation) did not change significantly. A possible explanation is that, since the bottom part of the bag leans on the picker legs (Figure 2 c), the α angle is largely determined by the body shape and posture; the lab experiments were done in the lab by subjects deliberately move their body in a “consistent” magnitude, as they pick, and therefore the weight of the bag does not affect significantly the α angle deviation.

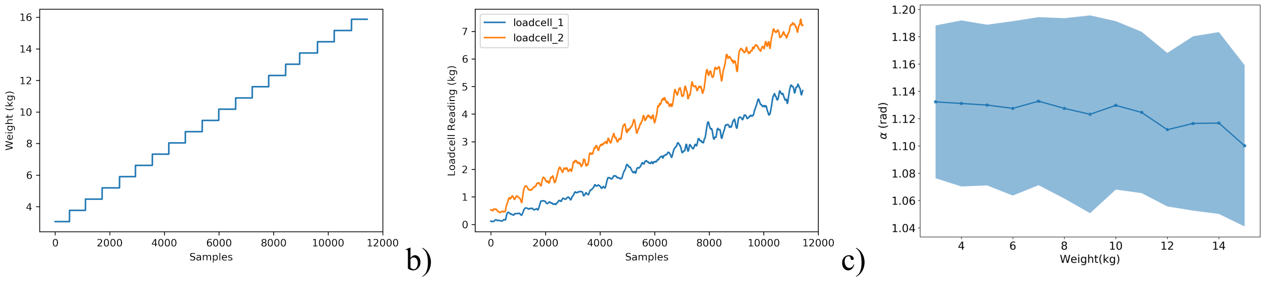

a) b) c)

Figure 6 a) Example of staircase weight signal (ground truth) when baseball batches of five were dropped in the bag. b) Corresponding load cell signals. c) Mean of the estimated α angle, and its standard deviation with respect to the load weight.

Validation datasets: Reference objects (baseballs) and fresh apple fruits single-drop datasets

The first validation dataset was collected using the same five-step procedure described above - for the calibration dataset – with one difference: one reference object (baseball) was added at a time (single-drop), instead of five objects. Adding one baseball at a time is closer to actual fruit picking, and was used to test the validity of the model. The second validation dataset was collected using fresh apples ('Red Delicious'); the average apple weight was measured to be 0.21 kg. A single-drop procedure was used to collect the real fruit dataset (one fruit at a time). Each fruit's weight was measured using a precision digital scale (L-EQ 10/20, Tor Rey Electronics Inc, Houston, TX, USA) and recorded before the fruit was dropped into the bag. One bag was filled for each of the validation datasets.

PERFORMANCE METRICS

The main performance metric used in this paper is the root mean square error (RMSE) between the predicted mass and the measured ground truth mass.

$$\mathrm{RMSE} = \frac{\sum_{i=1}^{n}(\hat{m}_i - m_i)}{n} \tag{24}$$

where $\hat{m}_i$ is the predicted mass and m_i is the ground truth mass at timestep sample i. The mean error, the standard deviation of error, and the 90th percentile of the absolute error are also used as supplementary error descriptive metrics.

REGRESSION AND VALIDATION

For the baseball batch-drop datasets, a cross-validation procedure was followed, i.e., the entire dataset was split into a training set and a validation set. The training set consisted of seven people's data, and the validation set was the remaining person's data. The cross-validation procedure was repeated eight times. Every person's data was used as a validation set. Regression (training) was performed on the training set, and validation was done on the validation set to get the performance indices. The errors for eight cross-validations were aggregated together to calculate the total estimation of performance for a specific regression model. The regression model from the batch-drop dataset was applied to the single-drop baseball and apple validation datasets. All load cell data were pre-filtered using a median filter of size 11 (which is about one second's data) to reject outliers from impulse noise/spikes.

Application Case Study: Apple-harvesting from an Orchard Platform

The purpose of this experiment is to demonstrate the functionality of the instrumented picking bags in real-world, commercial harvesting conditions. Two instrumented picking bags were calibrated in the lab and then used by two pickers to harvest Fuji apples, in a commercial apple orchard at Lodi, CA, on September 10, 2019. Trees were trained in a V-trellis architecture. The pickers were picking from a modified orchard platform (Bandit Xpress, Automated Ag Systems, Moses Lake, WA, USA), as shown in Figure 7.

a) b)

Figure 7 a) Two pickers harvesting on an orchard platform, using the instrumented bags. b) Close-up of a picker carrying his picking bag.

A Real-Time Kinematic GNSS receiver (Piksi Multi, Swift Navigation, San Francisco, CA, USA) with real-time corrections over a cellular network was mounted on the top of the platform to record position at cm-level accuracy. We harvested one side of a 50 m long tree row in the orchard. All the sensor data from the picking bags were transmitted to a computer on the platform in real-time. The sensor data was used for a) estimating each picker's bag weight at real-time; b) estimating the total weight of the fruit harvested so far by each picker by accumulating fruit weight - bag by bag; c) estimating individual worker's picking speed by calculating the average slope (increase rate) of the time series of the accumulated picked weight using a five-minute time window; d) estimating the yield distribution at a spatial resolution of three meters along one side of a tree row, by splitting the row's length into three-meter segments and calculating the total weight of the fruit picked by both pickers in each segment.

RESULTS AND DISCUSSION

CALIBRATION RESULTS FROM THE BASEBALL BATCH-DROP DATASET

Both models were calibrated with data from the baseball batch-drop experiments and then used to estimate/predict the weight of the baseballs in the calibration dataset. Figure 7 shows the ground truth and predicted weight signals from one randomly selected batch-drop dataset for models #1 and #2. The waveforms of the predictions of the two models in these graphs look similar (but are not identical), because they utilize the same load cell ground truth, and they are both reasonably accurate (they don't deviate much from ground truth). The error metrics in Table 1 show the overall cross-validation error statistics. The results indicate that model # 2's prediction fits the ground truth better than model #1 (it has 11.3% smaller 90^{th} percentile error). The calibrated model trained by all the available calibration data is saved on the device, and the model should remain valid, as long as the load cells are not changed, and the sensor installation positions don't change. Calibration needs to be done for each individual picking bag if the load cells are not pre-calibrated. If the load cells are pre-calibrated to the standard unit (kg), and the sensor installation positions are the same, the picking bag model can be shared across devices.

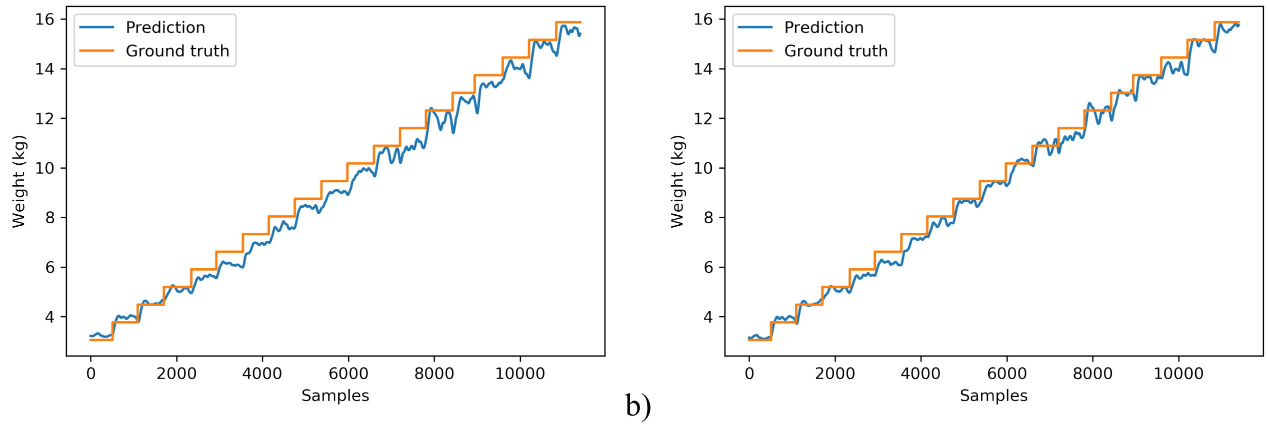

a) b)

Figure 8 Two examples of predicted vs. ground truth weight, during the baseball batch-drop experiments, using a) model #1, and b) model #2.

	Model #1	Model #2
RMSE (kg)	0.5463	**0.5038**
Mean |Error| (kg)	0.4206	**0.3898**
SD |Error| (kg)	0.3486	**0.3192**
|Error| 90% Percentile (kg)	0.9315	**0.8258**
RMSE /Bag Capacity(20kg)	2.732%	2.519%

Table 1 The overall cross validation error statistics of the baseball batch-drop dataset, for Models #1 and #2

RESULTS ON THE BASEBALL SINGLE-DROP VALIDATION DATASET

Both models were used to estimate/predict the weight of the baseballs in the single-drop validation dataset. Figure 9 a), b) show the ground truth and predicted weight signals of both models. The error metrics in Table 2 indicate that model #2 performed significantly better than model #1 (e.g., 55.93% less 90th percentile error). From Figure 9 c), we can see that the error tended to increase when the load increased, for both models; however, Model # 1's error increased more than the error of Model #2. Figure 9 d) shows that the relative error (error as a percentage of the load) increased for Model #1 but didn't increase much for Model #2. This can be attributed – to some extent – to the estimation and incorporation of angle α into model #2 (see section 7.3).

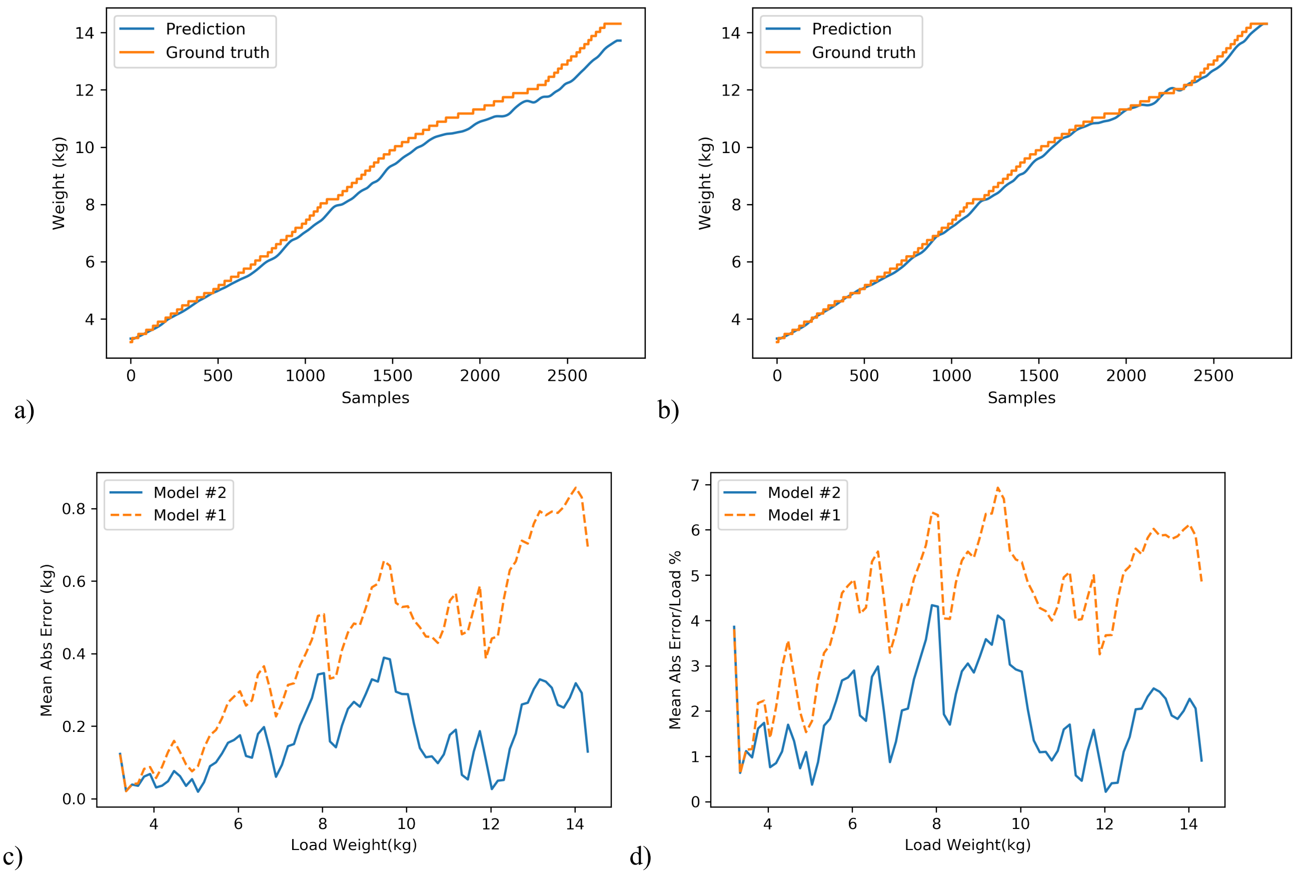

Figure 9 a) Predicted weight vs. ground truth weight for the baseball single-drop dataset, using Model #1. b) Predicted vs. ground truth weight for the baseball single-drop dataset, using Model #2. c) Mean absolute error vs. current load for the baseball single-drop dataset for both models. d) Corresponding mean absolute relative error (percentage of current load) for both models.

	Model #1	Model #2
RMSE (kg)	0.4679	**0.1899**
Mean |Error| (kg)	0.4118	**0.1560**
SD |Error| (kg)	0.2220	**0.1084**
|Error| 90% Percentile (kg)	0.7130	**0.3142**
RMSE /Bag Capacity(20kg)	2.340%	0.950%

Table 2 The overall cross-validation error statistics of the baseball single-drop dataset, for Models #1 and #2.

RESULTS FROM THE APPLE SINGLE-DROP VALIDATION DATASET

Both models were used to estimate/predict the weight of fresh apples in a single-drop validation dataset. Figure 10 a), b) shows the ground truth and predicted weight signals of both models. Figure 10 c) shows that the error increased with increasing load for both models; however, Model # 1's error increased more than Model #2 because Model #1 does not include α angle compensation. Figure 10 d) shows that the mean absolute relative error (% of the load) for Model #1 is always higher than that of Model #2. In the light-load range, we can see that both models have high relative errors; this is due to the fact that the total load is small, so the relative error is very sensitive to changes in the absolute error.

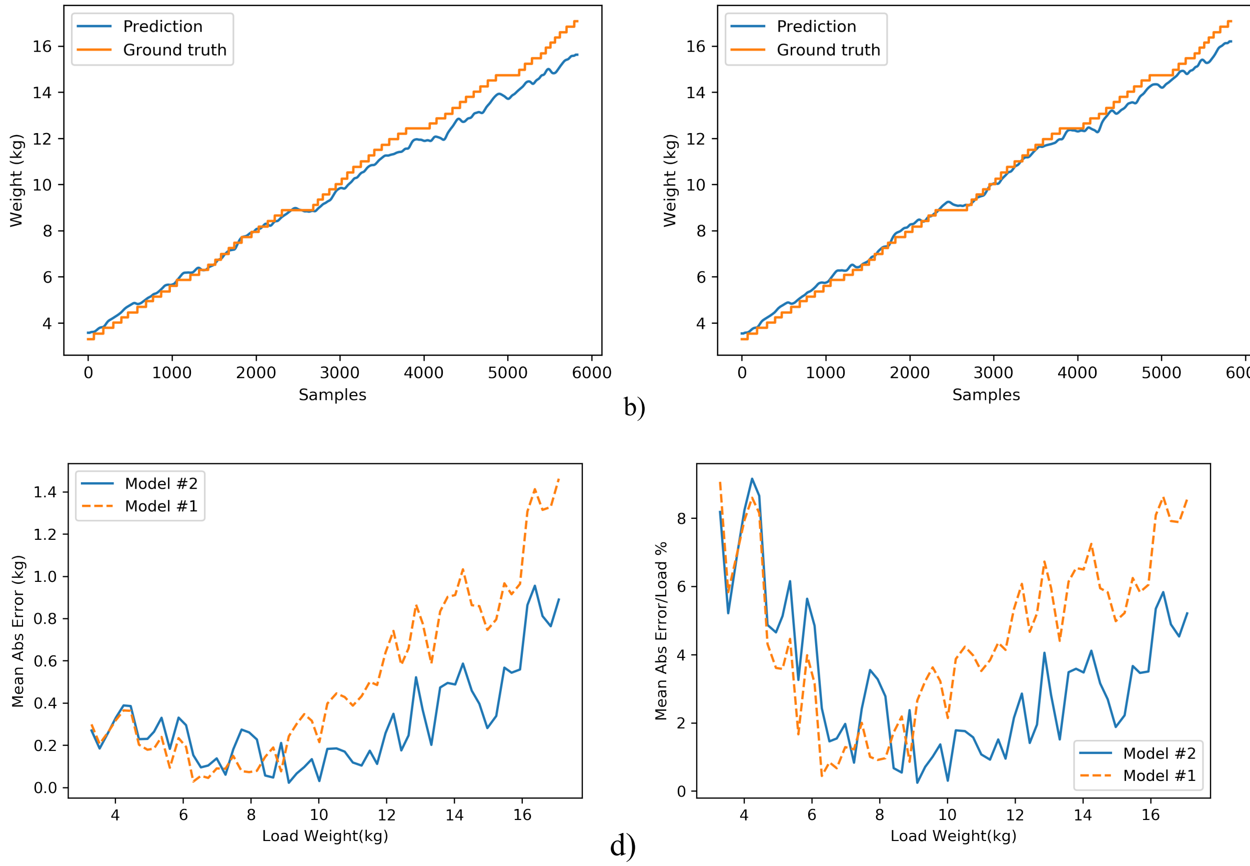

Figure 10 a) Predicted vs. ground truth weight for the apples single-drop dataset, using Model #1. b) Predicted vs. ground truth weight for the apple single-drop dataset, using Model #2. c) Mean absolute error vs. current load on the apples single-drop dataset, for both models. d) Corresponding mean absolute relative error (percent of current load) for both models.

	Model #1	Model #2
RMSE (kg)	0.5997	**0.3594**
Mean |Error| (kg)	0.4697	**0.2942**
SD |Error| (kg)	0.3729	**0.2064**
|Error| 90% Percentile (kg)	0.9609	**0.5566**
RMSE /Bag Capacity(20kg)	2.999%	1.797%

Table 3 The overall cross-validation error statistics of the apple single-drop dataset, for Models #1 and #2

From the above results, one can see that both models gave prediction RMSE less than 0.26 kg (which is less than the weight of one average-sized apple) in the light-weight range (< 8kg), when applied to the baseball and apple validation datasets. Figure 9 indicates that model #2 performed better than model #1 when the bag was heavier than 8 kg; model # 1's prediction started underestimating weight, whereas model # 2's prediction still predicted the ground truth closely. A possible explanation is that model #1 assumes that angle α doesn't change, whereas, in reality, it did (Figure 6 shows that angle α decreased – on average - as the load weight increased; model #2 incorporates the angle in the weight estimate. Most of the errors made by model #2 were within 0.5 kg, and the 90% percentile of the error was 0.56 kg, which was 42.08% less than the corresponding error of model #1.

Error distributions of both models for apple dataset

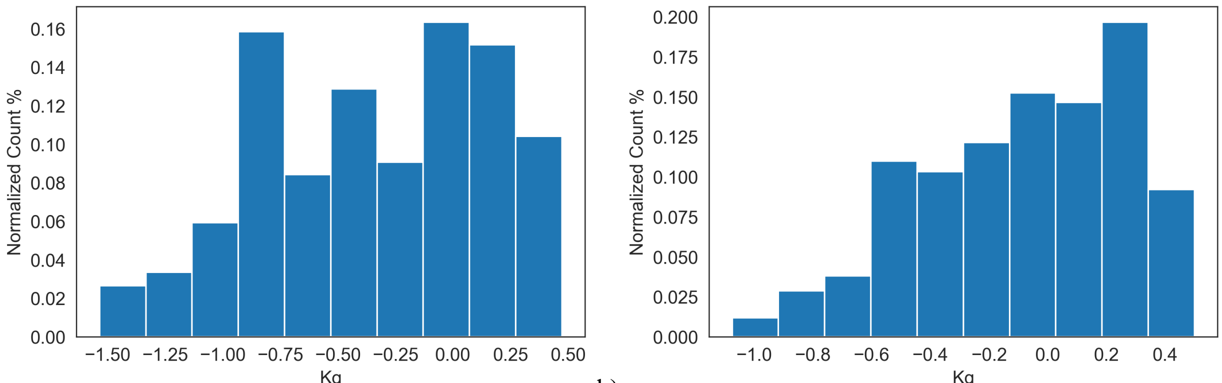

a) b)

Figure 11 a) Frequency histogram of fresh-apple weight error using model #1. b): Frequency histogram of fresh-apple weight error using model #2.

Figure 11 shows the frequency histograms of the errors of the two models; both distributions are biased toward negative errors(the mean error was -0.347 kg for model #1 and -0.088 kg for model #2), which means that both models tended to underestimate the true weight of the fruits in the bag. The underestimation effect was more significant in model #1, as it is also evident from Figure 10.

Errors in different ranges for apple dataset

To study the errors quantitatively under different load conditions, and gain insight into the performance of each model under varying load conditions, the total weight range was divided into three operating regions: light load (< 8kg), medium load (8-13kg), and heavy load (>13 kg).

	Model #1			Model #2		
	Light	Medium	Heavy	Light	Medium	Heavy
RMSE (kg)	**0.2189**	0.4573	0.9876	0.2595	**0.2250**	**0.5597**
Mean |Error| (kg)	**0.1825**	0.3862	0.9586	0.2429	**0.1827**	**0.5181**
SD |Error| (kg)	**0.1208**	0.2448	0.2374	0.1167	**0.1313**	**0.2118**
|Error| 90% Percentile (kg)	**0.3412**	0.7496	1.330	0.4061	**0.3553**	**0.8630**

Table 4 Error statistics in different load weight ranges (light load (< 8kg), medium load (8-13kg), and heavy load (>13 kg) for the apples single-drop dataset

The results indicate that the errors of both models, in the light and medium-load regions, were smaller than the overall error, and the errors in the heavy-load region were higher than the overall error. Model #1 performed slightly better than model #2 in the light-load region, whereas model #2 outperformed model #1 significantly, in the medium and heavy-load regions. One possible explanation why Model #2 had better performance in the medium and heavy-load regions, is that the angles α and β changed as loads became heavier. Model #1 did not incorporate any of these angles, and could not capture the effect of their change; hence, errors increased when the load increased. Model #2 captured the effect of changing α, so it performed better than model #1; still, it underestimated the fruit weight as the load increased, because it did not capture the effect of changing β. The possible reason that Model #1 outperformed Model #2 in the lightweight range is that although Model #2 utilized the α angle, the α angle estimation is based on a quasi-static-bag assumption (Eq.10 – Eq.12), which is not strictly true; hence, it seems that the error introduced by the violation of the quasi-static assumption was higher than the error introduced by not incorporating the angle at all, as in Model #1. The reason why the quasi-static assumption is violated in the light-weight region is that contact forces cause the bag to accelerated or decelerate more, and move at higher speeds, thus rendering the angle estimation less accurate. In the medium and heavy-weight ranges, the benefit of using the angle compensation is larger than the extra error introduced by α angle estimation error; thus, Model #2 performs better. Nonetheless, Model # 2's RMSE is 0.26 kg in the light-weight range, which is below the error over the full range.

The average weight of the 'Red Delicious' apple was measured to be 0.21 kg. Based on the mean absolute error of Model #2. This model can estimate the weight in the bag at 1-2 apple accuracy at the light and medium load and 2-3 apple accuracy at the heavy load range. The error at maximum load in the real apple experiment (16 kg, cannot put more apple in the bag) is 5.2%, which can be considered as the worst-case error in yield/picking rate estimation.

RESULTS OF THE COMMERCIAL APPLE-HARVESTING CASE STUDY

The data collected by the instrumented picking bags during commercial apple harvesting from a platform were used to calculate the picker productivities and yield information. The results are shown in Figure 12. Each picking bag's weight was estimated in real-time, as in Figure 12 a). The cumulative weight of the fruits harvested by each picker is shown in Figure 12 b). Individual worker picking speeds are shown in Figure 12 c). The apple yield distribution on the trees on the right side along the row is shown in Figure 12 d); the distribution is georeferenced and superimposed on a satellite image of the orchard. The productivity information shows the temporal variability in picker's picking rate, and the yield information shows the spatial variability in fruit distribution. They could be used for better labor and orchard management.

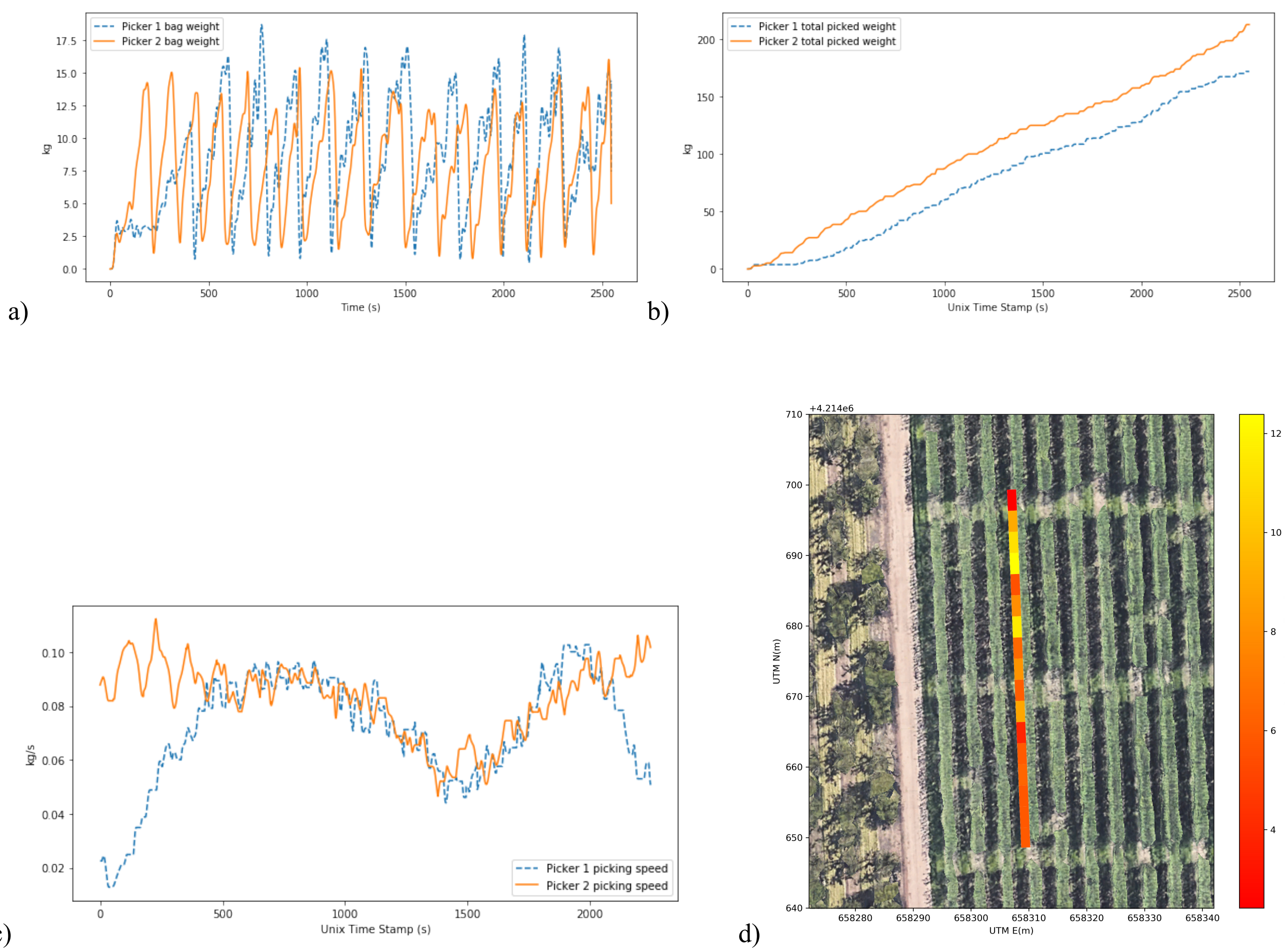

Figure 12 a) An example of two time-series of the pickers' estimated bag weights; b) The cumulative fruit weight harvested by each picker, as a function of time; c) The corresponding estimated fruit-picking speed of each picker; d) The corresponding estimated fruit density along the row, on one side of the trees (kg/m)

SUMMARY AND CONCLUSIONS

This paper reported the design, implementation, calibration, validation and real-world utilization of an instrumented fruit picking bag that can measure in real-time the weight of fruit harvested by a picker who carries and uses the bag to harvest. Two models were developed to predict true weight from load cell measurements. Model #1 used linear regression on the load cell values, whereas Model #2 used an IMU and incorporated the measurement of the bag angle that affects the projection of the true weight force onto the load cell measured forces. Overall, Model #2 was found to be more precise. The RMSE and 90th percentile errors of the weight predicted by Model #2 - in dynamic conditions - were less than 0.36 kg and 0.56 kg, respectively; these errors correspond to 1.8% and 2.8% of the bag capacity (20kg). Both models had higher errors when the fruit load was in the medium-to-full ranges. However, Model #2 had better performance in the heavy-load range. Two instrumented bags were used by two pickers to pick apples on a harvesting platform, during commercial harvesting. It was demonstrated that data from the bags could be used to estimate picker productivities and – in conjunction with a GPS – high-resolution yield maps. These results suggest data from the instrumented picking bags could be used for labor and orchard management.

A limitation of our commercial-harvesting case study is that ground truth data could not be collected, since the weights of the picked apples were unknown, and interrupting pickers regularly to weigh their bags with an accurate scale would alter the picking motions and signals; also, it was not acceptable by the grower and crew. Therefore, this case study was not used to validate the calibration models under real harvesting conditions.

Future work could apply each model in the load range it performs best to improve the overall performance. Also, a dynamic model that incorporates bag accelerations could be developed to better estimate bag weight under heavy loads. Finally, incorporation of a GPS receiver inside the electronics box – with a small external antenna - could enable the generation of high-resolution yield maps for all-manual harvesting (on ladders); however, it is expected that GPS signal availability would present a significant challenge for such applications

ACKNOWLEDGMENTS

This work was funded by NIFA grants 2016-67021-24535 and W3009 Hatch Multi-State 1016380.

Mr. Fei was partially supported by the China Scholarship Council (CSC).

REFERENCE

Aggelopoulou, K. D., Wulfsohn, D., Fountas, S., Gemtos, T. A., Nanos, G. D., & Blackmore, S. (2010). Spatial variation in yield and quality in a small apple orchard. Precision agriculture, 11(5), 538-556. http://doi.org/10.1007/s11119-009-9146-9

Ampatzidis, Y. G., Vougioukas, S. G., Bochtis, D. D., & Tsatsarelis, C. A. (2009a). A yield mapping system for hand-harvested fruits based on RFID and GPS location technologies: field testing. Precision agriculture, 10(1), 63-72. https://doi.org/10.1007/s11119-008-9095-8

Ampatzidis, Y. G., Whiting, M. D., Liu, B., Scharf, P. A., & Pierce, F. J. (2013). Portable weighing system for monitoring picker efficiency during manual harvest of sweet cherry. Precision agriculture, 14(2), 162-171. https://doi.org/10.1007/s11119-012-9284-3

Ampatzidis, Y., & Vougioukas, S. G. (2009b). Field experiments for evaluating the incorporation of RFID and barcode registration and digital weighing technologies in manual fruit harvesting. Computers and Electronics in Agriculture, 66(2), 166-172. https://doi.org/10.1016/j.compag.2009.01.008

Ampatzidis, Y., Tan, L., Haley, R., & Whiting, M. D. (2016). Cloud-based harvest management information system for hand-harvested specialty crops. Computers and Electronics in Agriculture, 122, 161-167. https: https://doi.org/10.1016/j.compag.2016.01.032

Beard, R. W., & McLain, T. W. (2012). Small Unmanned Aircraft: Theory and Practice. Princeton, NJ: Princeton university press.

Colaço, A. F., Trevisan, R. G., Karp, F. H., & Molin, J. P. (2015). Yield mapping methods for manually harvested crops. Precision agriculture '15 (pp. 39-44). Wageningen: Wageningen Academic Publishers.

Khosro Anjom, F., & Vougioukas, S. G. (2019). Online prediction of tray-transport request time using mechanistic grey box models for improved scheduling of robotic strawberry harvest-aids. Biosystems Engineering, 188, 265-287. https://doi.org/10.1016/j.biosystemseng.2019.10.025

Khosro Anjom, F., Vougioukas, S. G., & Slaughter, D. C. (2018). Development and application of a strawberry yield-monitoring picking cart. Computers and electronics in agriculture, 155, 400-411.

https://doi.org/10.1016/j.compag.2018.10.038

Khosro Anjom, K., Rehal, R. S., & Vougioukas, S. G. (2015). A Low-Cost, Efficient Strawberry Yield Monitoring System, ASABE Paper No. 152189408. St. Joseph, MI: ASABE. https://doi.org/10.13031/aim.20152189408

Lee, W. S., Burks, T. F., & Schueller, J. K. (2002). Silage Yield Monitoring System, ASABE Paper No. 021165. St. Joseph, MI: ASABE. https://doi.org/10.13031/2013.10382

Pelletier, G., & Upadhyaya, S. K. (1999). Development of a tomato load/yield monitor. Computers and Electronics in Agriculture, 103-117. https://doi.org/10.1016/S0168-1699(99)00025-3

Schueller, J. K., Whitney, J. D., Wheaton, T. A., Miller, W. M., & Turner, A. (1999). Low-cost automatic yield mapping in hand-harvested citrus. Computers and Electronics in Agriculture, 23(2), 145-153. https://doi.org/10.1016/S0168-1699(99)00028-9

Vatsanidou, A., Fountas, S., Nanos, G., & Gemtos, T. (2014). Variable Rate Application of Nitrogen Fertilizer in a commercial pear orchard. The International Journal of the American Farm School of Thessaloniki, 1, 1-8.

Zhang, Q. (2018). Automation in Tree Fruit Production: Principles and Practice. Boston, MA: CABI. https://doi.org/10.1079/9781780648507.0000

Zude-Sasse, M., Fountas, S., Gemtos, T. A., & Abu-Khalaf, N. (2016). Applications of precision agriculture in horticultural crops. https://doi.org/10.17660/eJHS.2016/81.2.2